Seismic fracture detection: ambiguity and practical solution

Ye Zheng, Dragana Todorovic-Marinic, Veritas DGC Inc., and Glenn Larson, Devon Canada Corp.*

Summary

It is becoming popular to extract fracture information from wide-azimuth P-P reflection seismic data. The extracted crack density is not influenced by the phase of the seismic data. The extracted fracture orientation is sensitive to the phase of seismic data and the nature of the rocks. Other information besides the amplitude and NMO velocity of seismic data is needed in order to uniquely determine the fracture orientation. This paper discusses the ambiguity of the fracture orientation and how it can be resolved. Todorovic-Marinic et al (2004) discussed the stabilization of crack density.

Introduction

Extracting fracture information from P-P reflection seismic data recently became a hot topic (Gray et al, 1999, 2000, Hall et al, 2000, Li, 1999, Lynn et al, 1996, MacBeth and Lynn, 2001). A fractured reservoir can be considered as an azimuthal anisotropic medium (or horizontally transverse isotropic medium). P and S wave velocities vary with the azimuth of the incident ray path. The amplitude and NMO velocity of reflected P waves vary with azimuth as well (Thomsen, 1988, Tsvankin, 1997). From the variation of the amplitude at different azimuths, one can extract crack density and orientation (Lynn et al, 1996). Practically, crack density extracted from seismic data is relatively stable. However, the extracted fracture orientation is sensitive to the phase of the seismic data and the types of geological interfaces.

The amplitude of reflected P wave on the interface between two azimuthal anisotropic media varies at different incident angles and azimuths of the ray path. The variation can be described as (Rüger, 2002):

$$R(\theta,\varphi) = A + [B^{iso} + B^{ani}\cos^2(\varphi - \varphi_{sym})]\sin^2\theta \qquad (1)$$

where R is the reflectivity (amplitude) of the P wave. A is the AVO intercept. B^{iso} is the isotropic AVO gradient. B^{ani} is the anisotropic gradient (crack density). θ is the incident angle of the seismic wave, φ is the azimuth of the ray path, and φ_{sym} is the azimuth of the direction perpendicular to the fracture strike. For a given offset (or incident angle), the amplitude variation curve is a sinusoid with a period of 180 degrees. There are four unknowns in the equation, A, B^{iso}, B^{ani} and φ_{sym}. Note that mathematically we can never get the unique solution from equation (1) no matter how much data are available. If we change the sign of B^{ani}, regroup B^{iso} and at the same time rotated φ_{sym} by 90 degrees, we can get another set of B^{iso}, B^{ani} and φ_{sym} that still satisfy the equation. One might force B^{ani} to be positive, but now the detected fracture orientation is questionable, because at the real world, B^{ani} could be positive or negative. Meanwhile, the above discussion is based on zero phase data and did not consider side lobes. When we deal with a seismic dataset with arbitrary phase and take the side lobes into account, things become more complicated.

The fracture orientation detected from azimuthal NMO velocity also has 90 degrees ambiguity. The NMO velocity for weak anisotropy at an arbitrary direction is given by Tsvankin (1997):

$$V_{nmo}^2 = V_0^2\,(1 + 2\delta^{(v)}\cos^2\alpha) \qquad (2)$$

Where V_0 is the NMO velocity along the fracture direction, α is the angle between fracture and seismic ray path. $\delta^{(v)}$ is the Thomsen parameter. In reality, $\delta^{(v)}$ can be either positive or negative. Unless we know the sign of $\delta^{(v)}$, we are facing the same problem as we have when using equation (1).

Synthetic tests

Synthetic datasets are created to test the fracture detection result with different phases of seismic data. The synthetic datasets are modeled using equation (1). This will give us some idea how the phase of the seismic data affects the results of fracture detection. The model has an isotropic layer on top of an anisotropic layer. A synthetic gather with a zero phase Ricker wavelet is created using equation (1). Then the gather is phase rotated by 30 degrees to create a series of gathers with different phases. Fracture detection is then applied to these gathers. In the inversion, B^{ani} is forced to be positive. Figure 1 shows the model and the results of fracture detection for different phases. Panel 8, on the far right side, is the model used for the test. The reflection interface is a Class I type interface (Rutherford & Williams, 1989) with positive intercept (A) and negative gradient (B^{iso}). The fracture orientation is set to 45 degrees (φ_{sym}) and the crack density (B^{ani}) is positive. The second panel from the right side (panel 7) is the result of fracture detection from the zero phase gather. On the far left side, panel 1, is the result of fracture detection from the 180 degrees phase-rotated (reversed

polarity) gather. By comparing panels 1 and 7, one can notice that the detected crack density is the same, but the fracture orientation is rotated by 90 degrees for each time sample. For each gather between 0 and 180 degrees, the detected fracture orientation is the same for some time samples and is rotated by 90 degrees for others. Looking at all panels from 1 – 7, one finds that the detected fracture orientation is rotated by 90 degrees wherever the intercept is negative. The average crack density over a wavelength remains same for the gathers rotated with different phases.

Now let's take a look at another synthetic example. A Class III type of interface is modeled. The same procedure was used as previous example. The results are shown in Figure 2. Similar to the previous case, when the phase of the input gather is rotated by 180 degrees, the detected fracture orientation is rotated by 90 degrees.

The average crack density over a wavelength is the same for all gathers, however in this case, the correct fracture orientation is detected when the AVO intercept is negative.

Other classes were tested using the same procedures as described above. From the results of the tests, one can find that the detected crack density is independent of the phase of the seismic gathers in terms of the average over a wavelet length. The detected fracture orientation rotates 90 degrees when the AVO intercept changes polarity. There is no specific tie between the polarity of AVO intercept and the correct fracture orientation.

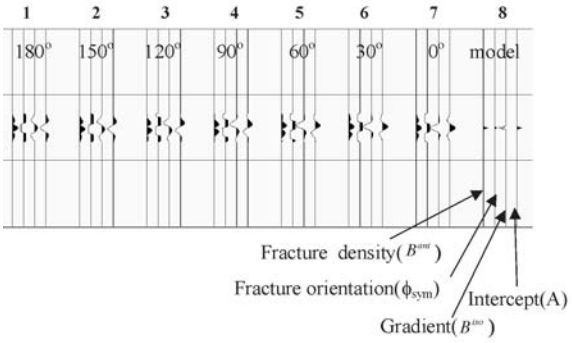

Figure 1. A Class I model (panel 8) is used to test the fracture detection result with different phases of seismic data. The model gather (not shown) is rotated by different amounts. The results of fracture detection for each rotation are shown in panels 1 – 7. The detected fracture orientation is correct when the AVO intercept is positive.

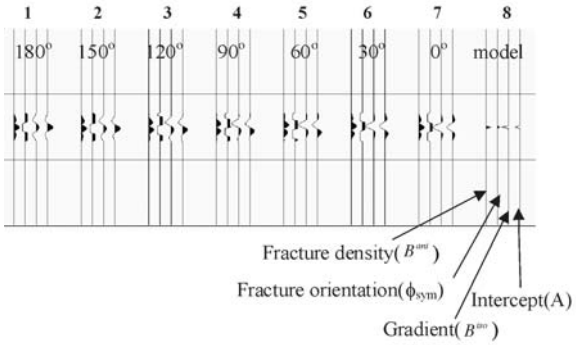

Figure 2. A Class III model (panel 8) is used to test the fracture detection result with different phases of seismic data. The model gather (not shown) is rotated by different amounts. The results of fracture detection for each rotation are shown in panels 1 to 7. The detected fracture orientation is correct when AVO intercept is negative.

Synthetic models were built to test the NMO velocity variation along azimuth. The models are composed of three layers with an azimuthally anisotropic layer in the middle. Eighteen (18) 2D lines were shot at different azimuths (every 10 degrees). The Thomsen parameter $\delta^{(v)}$ is positive in one model and negative in another. The reflections from the bottom of the fractured layer were NMO corrected using the average velocity. After NMO correction, the residual NMO (measured as time shift at a certain offset) was picked (Figure 3). The residual NMO from positive (blue) and negative (pink) $\delta^{(v)}$ both show sinusoidal pattern with a period of 180 degrees, but with opposite polarities, or 90 degrees phase off.

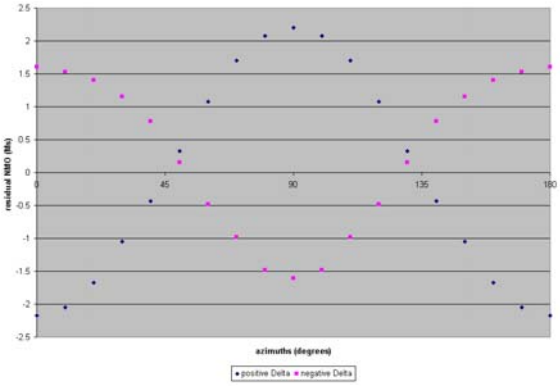

Figure 3. Residual NMO (measured as time shift at a certain offset) for the reflection from the bottom of the azimuthally anisotropic layer. The blue dots represent the residual NMO from the model with positive $\delta^{(v)}$, the pink dots for negative $\delta^{(v)}$. Both pink and blue dots show sinusoidal pattern, but with opposite polarities. The azimuth angle is measured from the symmetric axis (perpendicular to fracture).

Field data example

Copton 3D seismic dataset from the Narraway gas field in Alberta was used to test the impact of different phases of the seismic gathers on the detected fracture orientation. Fracture detection was applied to a region of 9x17 bins. The CMP bin size is 35 x 70m, with a test dimension of 630 x 595m. Figure 4 shows a stacked line in the middle of the test area (left) and three time slices of detected crack density and orientation (right). There is a short line in each CMP bin. The length of the bar represents the detected crack density and the direction of the bar represents the fracture orientation. The polarity of the stacked traces is negative for most CMPs at 1792 ms and positive at 1800 ms. The detected fracture orientations at 1792 ms are almost perpendicular to the fracture orientations at 1800 ms for most CMP bins. Since the data are from a structured area and the detected traces are from a group of CMPs, the detected fracture orientation at the two time levels may be not exactly off 90 degrees. At 1796 ms, some traces are on the positive side and some on negative side. Therefore the detected fracture orientations are close to what at the previous time sample (1792 ms) for some CMPs and the nest time sample (1800 ms) for others.

In order to solve the ambiguity of the detected fracture orientation, geological interpretation and well logging data were integrated. In Figure 5, the top (red) and bottom (purple) of the reservoir, Fahler G formation, are marked at the location of well 11-24. The detected fracture orientation at the top is -40^{o} and at the bottom, 50^{o}. FMI log tells that the fracture orientation in the Fahler G formation is 55^{o}. Therefore the orientation detected from seismic data is correct at the bottom and off 90^{o} at the top of the reservoir. The information from the interpretation of the FMI log solves the ambiguity. The contrast of crack density shows there are crack density changes at the top and bottom of the reservoir. The envelope method (Todorovic-Marinic et al 2003) will give better image of crack density.

Conclusions

The detected fracture orientation is not unique. It may be parallel or perpendicular to the fracture direction. In equation (1), if the crack density (B^{ani}) is forced to be positive, the fracture orientation from the inversion is sensitive to the phase of seismic data and the types of geological interfaces. The detected fracture orientation rotates 90 degrees when the AVO intercept polarity changes. There is no specific tie between the polarity of AVO intercept and the correct fracture orientation. When equation (2) is employed to detect fractures, the fast NMO velocity direction may not be the direction of the fracture. It depends on the sign of $\delta^{(v)}$. The addition of information besides the seismic amplitudes is required to resolve the ambiguity in the fracture orientation. In the case shown here, the FMI log helps solve the ambiguity of the detected fracture orientation.

Acknowledgements

The authors would like to take this opportunity to thank David Gray for the helpful discussions and Drs Michael Kendall and James Wookey of the University of Leeds, UK, for providing anisotropic modeling tool ATRAK.

References

Gray, F.D., Head, K.J., Chamberlain, C.K., Olson, G., Sinclair, J. and Besler, C., 1999, Using 3D Seismic to Identify Spatially Variant Fracture Orientation in the Manderson Field: SPE Paper 55636.

Gray, F.D. and Head, K.J., 2000, Fracture Detection in the Manderson Field: A 3D AVAZ Case History: The Leading Edge, Vol. 19, No. 11, 1214-1221.

Hall, S., Kendall, J.M., Barkved, O. and Mueller, M., 2000, Fracture characterization using P-wave AVOA in 3-D OBS data: 70th Ann. Internat. Mtg: Soc. Of Expl. Geophys., 1409-1412.

Li, X. -Y., 1999, Fracture detection using azimuthal variation of P-wave moveout from orthogonal seismic survey lines: Geophysics, Soc. of Expl. Geophys., **64,** 1193-1201.

Lynn, H.B., Simon, K.M. and Bates, C.R., 1996, Correlation between P-wave AVOA and S-wave traveltime anisotropy in a naturally fractured gas reservoir: The Leading Edge, 15, 8, 931-935.

MacBeth, C. and Lynn, H., 2001, Mapping fractures and stress using full-offset full-azimuth 3D PP data: 71st Ann. Internat. Mtg: Soc. of Expl. Geophys., 110-113.

Rüger, A., 2002, Reflection Coefficients and Azimuthal AVO Analysis in Anisotropic Media: Geophysical Monograph Series, Number 10, Soc. of Expl. Geophys.

Rutherford, S.R. and Williams, R.H., 1989, Amplitude-versus-offset variations in gas sands: Geophysics, 54, 680-688.

Thomsen, L., 1988, Reflection seismology over azimuthally anisotropic media: Geophysics, 53, 304-313.

Tsvankin, I., 1997, reflection moveout and parameter estimation for horizontal transverse isotropy: Geophyics, 62, 614 – 629.

Todorovic-Marinic, D., Gray, F.D., Zheng, Y., Larson, G. and Pelletier, J., 2003, Envelope of Fracture Density: Presented at the Joint CSEG/CSPG Convention.

Todorovic-Marinic, D., Larson, G., Gray, D., Soule, G., Zheng, Y. and Pelletier, J. 2004, Identifying vertical productive fractures in the Narraway gas field using the envelope of seismic anisotropy: presented at the CSEG convention.

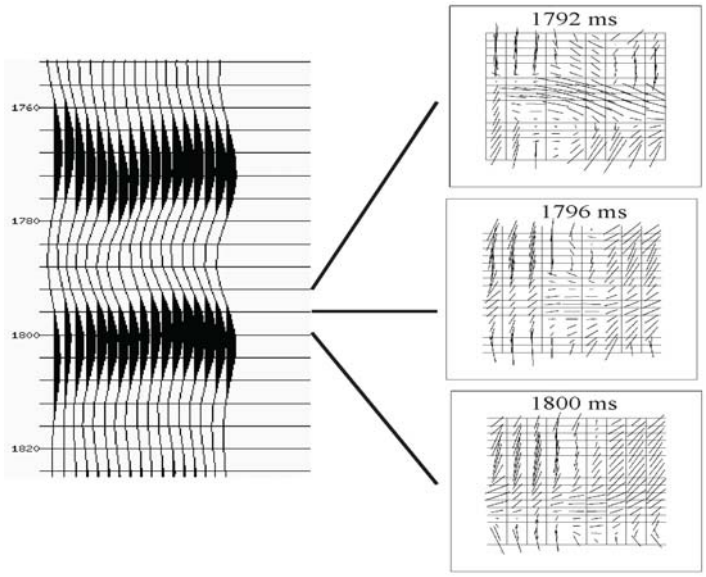

Figure 4. Three adjacent time slices of crack density and orientation detected from a seismic dataset in Alberta, Canada are shown on the right side. The length of the short lines in every CMP bin represents the crack density and the direction of the lines represents the fracture orientation. On the left side, it is a line of stacked section (in the middle of the test area). The detected fracture orientation rotates 90 ^{o} when the polarity of the stacked section changes.

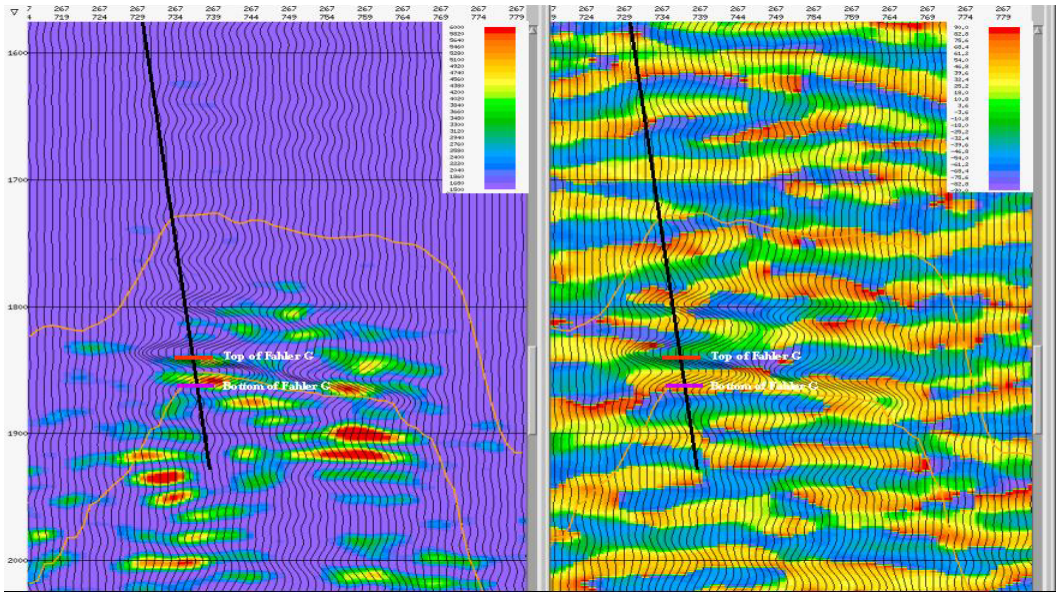

Figure 5. The left panel is P wave reflectivity (wiggle) overlaid by crack density contrast (color). The right panel is P wave reflectivity (wiggle) overlaid by fracture orientation (color). The top (red) and bottom (purple) of the reservoir (Fahler G) is marked on the well 11-24 (black tilted line). At the bottom of the reservoir, AVAZ gives correct fracture orientation. However, at the top of the reservoir, the orientation is 90^{o} off.